Research article

Poosan Muthu* and Vanacharla Pujitha

Effect of concentration dependence of viscosity on squeeze film lubrication

https://doi.org/10.1515/ZNA-2019-0370 Received December 19, 2019; accepted February 24, 2020; published online May 29, 2020

Abstract: The influence of concentration of solute particles on squeeze film lubrication between two poroelastic surfaces has been analyzed using a mathematical model. Newtonian viscous fluid is considered as a lubricant whose viscosity varies linearly with concentration of suspended solute particles. Convection-diffusion model is proposed to study the concentration of solute particles and is solved using finite difference method of Crank-Nicolson scheme. An iterative procedure is used to get the solution for concentration, pressure and velocity components in film region. It has been observed that load carrying capacity decreases as the concentration of solute particles in the fluid film decreases. Further, the concentration of suspended solute particles decreases as the permeability of the poroelastic plate increases and these results may be useful in understanding the mechanism of human joint.

Keywords: convection-diffusion model; poroelastic surface; squeeze film lubrication; variation of viscosity with concentration.

1 Introduction

Lubrication is a process by which friction and wear between two moving surfaces are reduced by a suitable substance called as lubricant. We can observe the lubrication process in machines, human body and other systems. Synovial joints are weight bearing systems in the human body with low frictional coefficient and wear in comparison with mechanical bearings [1].

Synovial joint is a connection between two moving bones consisting of a cartilage lined cavity filled with a lubricant called as synovial fluid. The behavior of synovial joint is mainly governed by the properties of synovial fluid and articular cartilage. The articular cartilage exhibits elastic behavior and is slightly permeable. The principal role of synovial fluid is to reduce friction between two moving articular cartilage surfaces. Its viscosity is due to the presence of hyaluronic acid (HA) molecules in it. In normal joints, these acid molecules cannot pass through the articular cartilage [2].

Torzilli and Mow [3] studied theoretically the characteristics of articular cartilage and synovial fluid. Bujurke et al. [4] have analyzed the squeeze film lubrication of synovial joint using a mathematical model by considering the lubricant as second-order fluid and cartilage as a porous surface. Hou et al. [5] have studied the lubrication mechanism of articular cartilage. Squeeze film lubrication of synovial joint with Bingham fluid as a lubricant and cartilage as a two layered porous region is mathematically modeled by Tandon et al. [6]. Bujurke and Kudenatti [7] have studied the effect of surface roughness and poroelastic behavior of cartilage on lubrication mechanism of joint. From all these research articles one can observe that load carrying capacity and pressure are important physical quantities in the study of lubrication mechanism. These quantities decrease with increasing values of permeability of the porous surface and increase with increasing values of elastic parameter.

Walker et al. [8] proposed the concept of boosted lubrication in load bearing phase of synovial joint. It is mentioned that when two bones approach each other, water and low molecular weight molecules pass through the cartilage surface and the HA molecules remain in the joint cavity. Due to the presence and increase in the concentration of acid molecules, the joint supports more load. Tannin et al. [9] experimentally investigated that presence of HA in synovial fluid reduces coefficient of

^{*}Corresponding author: Poosan Muthu, Department of Mathematics, National Institute of Technology, Warangal, 506004, Telangana, India, E-mail: pm@nitw.ac.in

Vanacharla Pujitha: Department of Mathematics, National Institute of Technology, Warangal, 506004, Telangana, India

friction in joint. Collins [10] analyzed the gel formation of HA molecules in joint. Tandon et al. [11] studied the lubricant gelling in synovial joint during articulation with viscoelastic fluid as lubricant. Mathematical model on dispersion of acid molecules and nutrients transport in the articular cartilage is useful in understanding the mechanism of synovial joint [12]. These studies modeled the effect of HA molecules on joint mechanism, assuming constant viscosity coefficient. But, the coefficient of viscosity of the synovial fluid changes with concentration of acid molecules present in it.

Recently, studies have been carried out to model the synovial fluid flow in rectangular cavity [13, 14]. In these investigations, the following assumptions are made: (i) viscosity depends on concentration and shear rate and (ii) shear-thinning index depends on concentration. But, geometry considered in the study is not relevant to biological synovial joint. That is, surfaces are rigid and flat. In nature, the joint surfaces are poroelastic. Further, the effect of concentration of HA molecules on pressure and load carrying capacity is not investigated in these articles.

Morris et al. [15] reported that the viscosity of synovial fluid increases rapidly and exponentially with concentration of HA molecules. Mathematical model describing the combined effect of variation of viscosity with concentration of HA and poroelastic nature of cartilage surface on lubrication of joint is not available in the literature. Hence, the main purpose of the present paper is to study the effect of concentration of solute particles on squeeze film lubrication between two poroelastic surfaces, assuming variable viscosity coefficient with respect to concentration.

2 Mathematical formulation

Figure 1 is the geometrical representation of model of synovial joint under consideration along with cartesian coordinate system (x, z), where x and z are parallel and perpendicular to the plates, respectively. According to Walker and Erkman [16], the load bearing area of the synovial knee joint is small under loading conditions. Therefore, two articular surfaces may be considered to be parallel. The x- axis is taken as middle of the channel. Let 2L be the length of the plates, 2h be the thickness of the film region and δ be the thickness of the poroelastic region. Upper poroelastic surface is moving normally with constant velocity dh/dt towards fixed poroelastic surface.

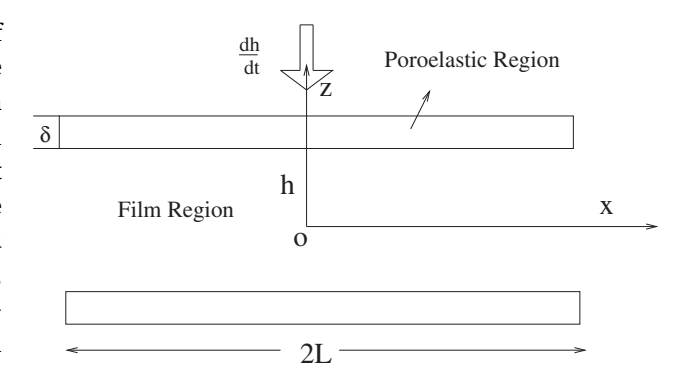


Figure 1: Geometry of the present problem.

The assumptions involved in mathematical formulation of the problem are listed below: In the film region, Newtonian viscous fluid is taken as lubricant, whose viscosity varies with concentration of HA. Fluid flow is laminar. Body forces are neglected. Fluid inertia is small compared to viscous shear. The height of the fluid film h is very small compared to the length L. Since squeeze film thickness is smaller than the length of the plates, variation of pressure across the fluid film is insignificant. Compared with the velocity gradient $\partial u/\partial z$ all other velocity gradient are considered negligible. Since *u* is predominant velocity and *z* is a dimension smaller than x. Thus the velocity gradient $\partial u/\partial z$ is large compared with all other velocity gradients. Therefore, the differential of the product of viscosity and the derivative $\partial u/\partial z$ with respect to z dominate the viscous term and remaining all derivatives are neglected. Based upon these assumptions as given in [17], the governing equations for the fluid flow in the film region are as follows:

Film region:

$$\frac{\partial u}{\partial x} + \frac{\partial w}{\partial z} = 0 \tag{1}$$

$$\frac{\partial p}{\partial x} = \frac{\partial}{\partial z} \left[\mu \frac{\partial u}{\partial z} \right]$$
 (2)

$$\frac{\partial p}{\partial z} = 0 \tag{3}$$

$$u\frac{\partial c}{\partial x} + w\frac{\partial c}{\partial z} = D\frac{\partial^2 c}{\partial z^2}$$
 (4)

where u and w are velocity components in the film region along x and z directions, respectively. p is fluid film pressure, μ is the coefficient of viscosity. c is concentration of solute particles and D is diffusion coefficient.

Ferguson et al. [19] experimentally proved that the viscosity of the synovial fluid linearly depends on concentration of HA. Accordingly, we assume that the coefficient of viscosity (μ) depends upon the concentration, as given in the following expression [2, 19],

$$\mu = \mu_0 \left(1 + \lambda c \right) \tag{5}$$

where λ is constant and μ_0 is viscosity of fluid entering poroelastic region.

In poroelastic region, the fluid is assumed to be Newtonian fluid with constant viscosity μ_0 . Coupled governing equations of fluid flow in deformable cartilage matrix can be written as in [3, 18].

Poroelastic region:

Matrix:
$$\rho_m \frac{\partial^2 \vec{U}}{\partial t^2} = div(\sigma_m) - \frac{\mu_0}{k} \left(\frac{\partial \vec{U}}{\partial t} - \vec{V} \right)$$
 (6)

Fluid:
$$\rho_f \frac{\overrightarrow{DV}}{Dt} = div(\sigma_f) + \frac{\mu_0}{k} \left(\frac{\partial \overrightarrow{U}}{\partial t} - \overrightarrow{V} \right)$$
 (7)

where \overrightarrow{U} is displacement vector of the cartilage, ρ_f and ρ_m are the densities of fluid and cartilage respectively. k is permeability of the cartilage and *V* is fluid velocity vector in cartilage. The stress tensors σ_m and σ_f for cartilage and fluid respectively, may be expressed as below

$$\sigma_m = p'I + 2Ne + AeI \tag{8}$$

$$\sigma_f = -p'I + EeI \tag{9}$$

where N, E and A are elastic parameters of the cartilage, p'is the fluid pressure in the cartilage, e is cartilage dilatation and *I* is the identity tensor. Inertial terms are neglected in the Eqs (6) and (7) due to the physical reasons and the corresponding order of magnitude analysis as mentioned in [7, 19]. Then we have,

$$\operatorname{div}(\sigma_m) - \frac{\mu_0}{k} \left(\frac{\partial \overrightarrow{U}}{\partial t} - \overrightarrow{V} \right) = 0 \tag{10}$$

$$\operatorname{div}(\sigma_f) + \frac{\mu_0}{k} \left(\frac{\partial \vec{U}}{\partial t} - \vec{V} \right) = 0 \tag{11}$$

Adding Eqs (10) and (11) and using Eqs (8) and (9), we

$$\nabla e = 0 \tag{12}$$

The divergence of Eq. (12) gives

$$\nabla^2 e = 0 \tag{13}$$

We define cartilage dilatation in terms of average bulk modulus K as given in [20],

$$e = e_0 + \frac{p'}{K} \tag{14}$$

We get equation of pressure in poroelastic region by substituting Eq. (14) in (13) as,

$$\nabla^2 p' = 0 \tag{15}$$

Next, we will derive the equation corresponding to the pressure in film region, using velocity components u and w. For which, the governing Eqs (1) and (2) are solved to get solution for u and w, using suitable boundary conditions as given below.

Boundary conditions:

The boundary conditions for velocity field are:

i. At the axis of symmetry:

$$\frac{\partial u}{\partial z} = 0$$
 and $w = 0$ at $z = 0$. (16)

ii. At the permeable wall, the tangential velocity (u) is zero. That is, no-slip boundary condition is applied. The normal velocity (w) of fluid in the film region is equal to normal component of the relative fluid velocity (w_n) at the cartilage surface and velocity of the upper moving plate (dh/dt), as given below [1]:

$$u = 0$$
 and $w = -w_n - \frac{dh}{dt}$ at $z = h$. (17)

The boundary conditions for concentration of solute particles in fluid film region are:

i. At middle of the channel (x = 0), as height h decreases, the solute concentration increases uniformly about that cross-section [10]. That is,

$$c = \frac{c_0 h_0}{h}$$
 at $x = 0$, (18)

where c_0 is the uniform solute concentration value when initial height is h_0 .

ii. At the symmetry plane:

$$\frac{\partial c}{\partial z} = 0 \quad \text{at } z = 0. \tag{19}$$

iii. Solute mass flux at the permeable wall is given by [21]:

$$-D\frac{\partial c}{\partial z} = h^* \left(c - c_p \right) + (T_h - 1) w_n c \quad \text{at } z = h, \tag{20}$$

where c_p is the concentration inside the poroelastic region, h^* is permeability of solute at the wall and T_h is transmittance factor. T_h is defined as the fraction of the solute present at the interface, which actually enters the pores of the surface and which gets transferred through it by bulk flow [21].

The solute flux through the interface is given by the boundary condition (20). The solute flux by diffusion process is given by product of permeability of solute at the wall (h^*) and transmembrane concentration difference $[c(z = h) - c_n]$. The solute flux by bulk flow is given by $(T_h - 1)w_nc$.

3 Solution

Solution of velocity component (u) is obtained by integrating the x- momentum Eq. (2), twice with respect to zand applying the boundary conditions (16) and (17). It is expressed as:

$$u = \frac{\partial p}{\partial x} \int_{h}^{z} \left(\frac{z}{\mu}\right) dz. \tag{21}$$

Solution of normal velocity component (w) is obtained by substituting the velocity u in the continuity Eq. (1) and integrating it with respect to z. Further, applying boundary condition (16) on w and following Leibnitz rule, we get,

$$w = \frac{\partial}{\partial x} \left\{ \int_{z}^{0} \left[\frac{\partial p}{\partial x} \int_{h}^{z} \left(\frac{z}{\mu} \right) dz \right] dz \right\}. \tag{22}$$

Substituting the velocity component *u* in the continuity Eq. (1) and integrating it over the film thickness from z = 0to z = h with respect to z using boundary conditions (16) and (17) of w, we get Reynolds equation as below,

$$\frac{\partial}{\partial x} \left\{ \int_{0}^{h} \left[\frac{\partial p}{\partial x} \int_{h}^{z} \left(\frac{z}{\mu} \right) dz \right] dz \right\} = w_{n} + \frac{dh}{dt}$$
 (23)

After neglecting the inertia term in Eq. (7), we have

$$\frac{\partial \overrightarrow{U}}{\partial t} - \overrightarrow{V} = \frac{k}{\mu_0} \left(- \nabla p' + E \nabla e \right) \tag{24}$$

Substitution of Eq. (14) in Eq. (24), gives

$$\frac{\partial \overrightarrow{U}}{\partial t} - \overrightarrow{V} = \frac{k}{\mu_0} \nabla p' \left(1 - \frac{E}{K} \right)$$
 (25)

Now w_n can be defined as

$$w_n = \text{normal component of}\left(\frac{\partial \overrightarrow{U}}{\partial t} - \overrightarrow{V}\right) = \frac{k}{\mu_0} \left(1 - \frac{E}{K}\right) \frac{\partial p'}{\partial z}\Big|_{z=h}$$
(26)

Integrating the Laplace Eq. (15) with respect to z over porous matrix thickness from z = h to $z = h + \delta$ and using boundary condition $\partial p'/\partial z = 0$ at $z = h + \delta$, we get

$$\frac{\partial p'}{\partial z}\Big|_{z=h} = \int_{h}^{h+\delta} \frac{\partial^{2} p'}{\partial x^{2}} dz$$
 (27)

If the thickness of porous layer (δ) is assumed to be of very small then Eq. (27) reduces to

$$\left. \frac{\partial p'}{\partial z} \right|_{z=h} = \delta \frac{\partial^2 p}{\partial x^2} \tag{28}$$

Eq. (28) is valid in the limiting case when $\delta \approx 0$ (see reference [22]).

Therefore,

$$w_n = \frac{k}{\mu_0} \delta \left(1 - \frac{E}{K} \right) \frac{\partial^2 p}{\partial x^2}$$
 (29)

Substituting Eq. (29) in Reynolds Eq. (23), we get equation for pressure in film region as,

$$\frac{\partial}{\partial x} \left\{ \frac{\partial p}{\partial x} F(x) \right\} = \frac{dh}{dt} \tag{30}$$

where
$$F(x) = \int_{0}^{h} \left(\int_{h}^{z} \left(\frac{z}{\mu} \right) dz \right) dz - \frac{k}{\mu_0} \delta \left(1 - \frac{E}{K} \right)$$

Solution for pressure in the film region can be obtained by solving Eq. (30) along with boundary conditions given below.

Boundary conditions for Pressure:

i. At middle of the channel:

$$\frac{dp}{dx} = 0 \quad \text{at } x = 0. \tag{31}$$

ii. At end of the channel:

$$p = 0 \quad \text{at } x = L. \tag{32}$$

Integrating Eq. (30) with respect to x twice and using boundary conditions (31) and (32) we get pressure in the dimensional form as,

$$p = \frac{dh}{dt} \int_{L}^{x} \frac{x}{F} dx \tag{33}$$

We define the following non-dimensional quantities

$$\overline{x} = \frac{x}{L}$$
, $\overline{z} = \frac{z}{h_0}$, $\overline{h} = \frac{h}{h_0}$, $\overline{u} = \frac{u}{dh/dt}$

$$\overline{w} = \frac{w}{dh/dt}$$
, $\overline{w}_n = \frac{w_n}{dh/dt}$, $\psi_0 = \frac{k\delta}{h_0^3}$, $\overline{p} = \frac{ph_0^3}{\mu_0 L^2 (dh/dt)}$,

$$l = \frac{L}{h_0}$$
, $\overline{c} = \frac{c}{c_0}$, $\overline{c}_p = \frac{c_p}{c_0}$, $\overline{\mu} = \frac{\mu}{\mu_0}$

to get the dimensionless form of the Eqs (4), (5), (21), (22) and (33).

We get the non-dimensional pressure in the film region as, after dropping bar,

$$p = \int_{1}^{x} \frac{x}{F} dx \tag{34}$$

where
$$F = \int_{0}^{h} \left(\int_{h}^{z} \left(\frac{z}{\mu} \right) dz \right) dz - \psi_{0} \left(1 - \frac{E}{K} \right)$$

The convection diffusion Eq. (4) and corresponding initial and boundary conditions (18), (19) and (20) are written in non-dimensional form (after removing bar) as:

$$Pe\left[u\frac{\partial c}{\partial x} + w\frac{\partial c}{\partial z}\right] = \frac{\partial^2 c}{\partial z^2},\tag{35}$$

$$c = \frac{1}{h} \quad \text{at } x = 0 \tag{36}$$

$$\frac{\partial c}{\partial z} = 0 \quad \text{at } z = 0 \tag{37}$$

and
$$\frac{\partial c}{\partial z} = Sh(c_p - c) + Pe(1 - T_h)w_nc$$
 at $z = h$, (38)

where $Pe = (dh/dt) h_0/D$ is the Peclet number and $Sh = h^* h_0/D$ is Sherwood number.

Non-dimensional form of velocity components and viscosity (after removing bar) are

$$u = \frac{\partial p}{\partial x} \int_{h}^{z} \left(\frac{z}{\mu}\right) dz \tag{39}$$

$$w = \frac{\partial}{\partial x} \left\{ \int_{z}^{0} \left[\frac{\partial p}{\partial x} \int_{h}^{z} \left(\frac{z}{\mu} \right) dz \right] dz \right\}$$
 (40)

and
$$\mu = 1 + \lambda c_0 c$$
 (41)

Now, we solve Eq. (35), which is coupled with Eqs (34), (39), (40) and (41). It is not possible to solve the Eq. (35) analytically, along with u, v and p quantities. Hence, Eq. (35) is solved numerically along with initial and boundary conditions (36), (37) and (38), in an iterative manner.

3.1 Numerical procedure

Finite difference method of Crank-Nicolson scheme is used to solve the convection-diffusion Eq. (35) along with the initial and boundary conditions (36)-(38), to get concentration value c(x, z). Trapezoidal procedure is used to evaluate integrals appearing in the solutions for pressure (p) and velocity components (u) and (w). Let the channel middle (x = 0) and outlet (x = 1) be denoted by index i = 0 and i = M, respectively. Similarly, the bottom (z = 0) and the top (z = h) are represented by index j = 0and i = N. Assume that Δx and Δz are increments in x and zdirections, respectively. The discretized form of solute transport Eq. (35) at a general grid point with indices (i, j)can be written as,

$$A_j \, c_{i+1,j-1} + B_j \, c_{i+1,j} + E_j \, c_{i+1,j+1} = R_j, \, for \, 0 < i \le M, \, 0 \le j < N$$
 (42)

where coefficients A_i , B_i , E_i and R_i are given by

$$A_{j} = -Pe \frac{\Delta x}{\Delta z} w_{i+1,j} - 2r,$$

$$B_{j} = 2Pe \left[u_{i,j} + u_{i+1,j} \right] + 4r,$$

$$E_{j} = Pe \frac{\Delta x}{\Delta z} w_{i+1,j} - 2r,$$

$$R_{j} = \left[Pe \frac{\Delta x}{\Delta z} w_{i,j} + 2r \right] c_{i,j-1} + \left[2Pe \left(u_{i,j} + u_{i+1,j} \right) - 4r \right] c_{i,j} + \left[-Pe \frac{\Delta x}{\Delta z} w_{i,j} + 2r \right] c_{i,j+1}$$
and $r = \frac{\Delta x}{(\Delta z)^{2}}$

To obtain the solute concentration value at the symmetric plane (z = 0), we use discretized form of Eq. (37) along with (42). That is, at z = 0, we have

$$B_0 c_{i+1,0} + E_0 c_{i+1,1} = R_0, \text{ for } 0 < i \le M$$
 (43)

where
$$B_0 = 2Pe[u_{i,0} + u_{i+1,0}] + 4r$$
, $E_0 = -4r$

and
$$R_0 = \left[2Pe(u_{i,0} + u_{i+1,0}) - 4r\right]c_{i,0} + 4rc_{i,1}$$

To calculate solute concentration values at top boundary, we discretize the boundary condition (38) by using three point backward difference formula [23]. Hence, at z = h, we have

$$c_{i,n} = \frac{4c_{i,n-1} - c_{i,n-2} + 2\Delta zShc_p}{3 + 2\Delta z(Sh + (T_a - 1)Pew_n)}, \text{ for } 0 < i \le M$$
 (44)

Thomas algorithm is used to solve the system of linear Eqs (42)–(44). The solutions for concentration (c), velocity components (u, w) and pressure (p) are obtained using an iterative procedure.

Solution procedure is started by assuming an approximate value for c, say $c_{i,j}^0$, for grid points with indices (i = 1 to M and j = 0 to N). At i = 0 level, p, u, w and c are known values. The approximate c values need to be corrected based upon Eqs. (34), (35) and (39)–(41) by satisfying the boundary conditions (37) and (38). The assumed c values are used to get approximate solutions for p, u and w, which are calculated from Eqs. (34), (39) and (40). Now, new c, say $c_{i,j}^1$, values are calculated from Eq. (42) along with boundary conditions (43) and (44). Using these new c values, new p, uand w are calculated. This algorithmic procedure is repeated until $|c_{i,i}^{n+1} - c_{i,i}^n| \le 10^{-6}$.

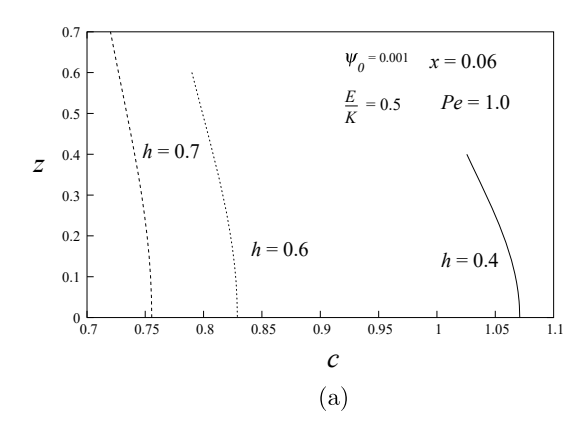
Once the correct *c* value for all grid points is obtained, then the fluid viscosity and the squeeze film pressure are calculated numerically using Eqs. (41) and (34), respectively. Further, the non-dimensional form of load carrying capacity can be obtained by integrating this pressure p over the film region. It is expressed as:

$$W = \int_{0}^{1} p \, dx \tag{45}$$

4 Results and discussion

The objective of this analysis is to study the effect of solute concentration on squeeze film lubrication between two poroelastic surfaces. This study may be useful in understanding the lubrication mechanism of joint due to the following reason When the articular cartilages move closer to each other, water and low molecular solutes may press out from joint cavity into cartilage surface. As a result, the concentration of HA molecules increases in the film region which supports more load [24].

The computational results are obtained for solute concentration (c), squeeze film pressure (p) and load carrying capacity (W). The parameters of interest in this paper are film height h, permeability parameter ψ_0 and elastic



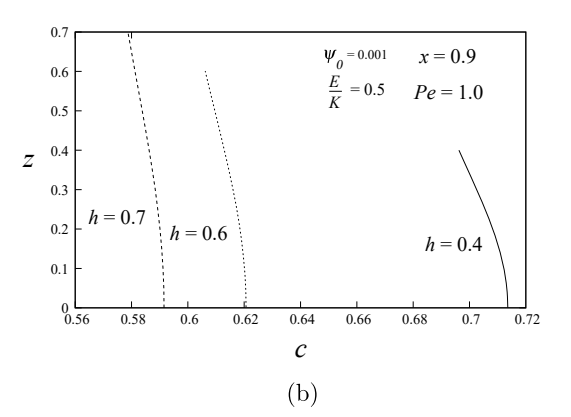


Figure 2: Distribution of concentration c with z at different cross sections (a) x = 0.06 and (b) x = 0.09.

parameter E/K. Effect of these parameters on c, p and W are discussed. Further, we have fixed Sh = 0.3, $c_p = 0.5$ and $T_a = 0.8$ throughout the analysis.

Solute concentration (c(x, z)):

Figure 2(a) depicts the influence of squeeze film height (h) on the distribution of concentration of solute particles (c) along normal direction z at cross section x = 0.06, for ψ_0 = 0.001 and E/K = 0.5. It is clear that there is an increase in the value of concentration of the solute particles as the height between two surfaces decreases. Also, the profile of c is obtained at cross section x = 0.9, and is given in Figure 2(b). Similar trend is observed as in Figure 2(a), with a quantity difference. This may be illustrated that in normal synovial joint(low permeability), as the height becomes smaller, the fluid squeezes through the cartilage surfaces and HA molecules remain in the joint cavity [8, 11, 24–26]. Hence, as the height decreases, concentration increases in the film region.

Figure 3 shows the distribution of concentration calong normal direction z for various values of permeability of the poroelastic surface ψ_0 at cross section x = 0.06, at fixed height h = 0.4. The concentration of solute particles decreases in the film region with increase in values of ψ_0 . This may be interpreted as that, in diseased joint, the articular cartilage becomes softer and has more permeability. As a result of this, more voids are available in the poroelastic surface. In such case, acid molecules can pass through the articular cartilage during joint movement, hence, concentration of solute particles decreases as ψ_0 increases [2]. Further, it is observed in the experimental work of Temple et al. [27] that the concentration of HA differed between diseased and normal synovial fluid in a manner that varied with molecular weight and HA concentration in diseased synovial fluid to normal case was lower in the large molecular weight range. Dahl et al. [28] also reported that there are reduced HA concentration in synovial fluids from rheumatoid arthritis patients.

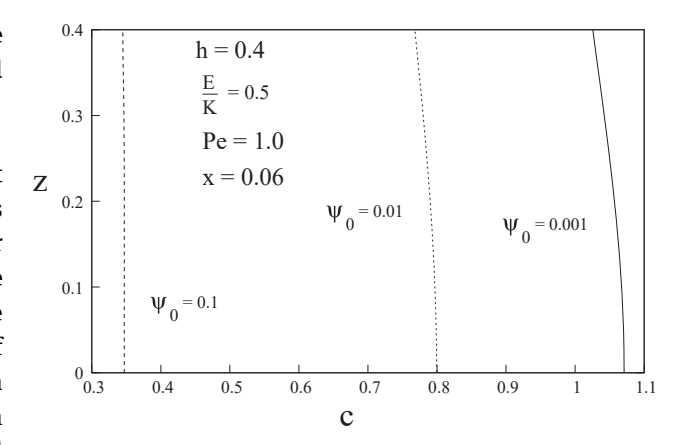


Figure 3: Distribution of concentration *c* with *z* for different values of ψ_0 .

Effect of elastic parameter E/K on the distribution of c varying with z at cross section x=0.06 is presented in Figure 4. It is observed that, the concentration c increases for increasing values of $\frac{E}{K}$. The values of E/K for normal and degenerative articular cartilage are 0.6 and 0.2, respectively, as remarked in the experimental study [20]. The degenerative cartilage surface is characterized by increasing porosity, permeability and decreasing stiffness [3]. If E/K=0.6, then, the cartilage surface has more stiffness than the surface with E/K=0.2. Hence, joint with degenerative cartilage has less solute particles movement during joint motion.

Figure 5 illustrates the influence of Peclet number Pe on the distribution of concentration c at cross section x = 0.06. It is understood that c increases as Pe increases. It may be interpreted as that there is a significant effect of convection term on the distribution of concentration of solute particles in squeeze film lubrication.

Solute concentration at interface (c_i) :

Figure 6 represents axial distribution of solute concentration (c_i) at the interface for various squeeze film heights, for $\psi_0 = 0.001$. It is seen that, c_i increases as h decreases for small value of $\psi_0 = 0.001$.

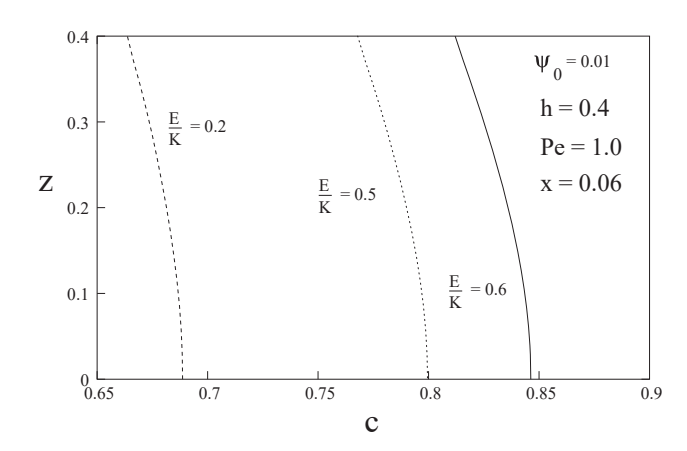


Figure 4: Distribution of concentration c with z for different values of E/K.

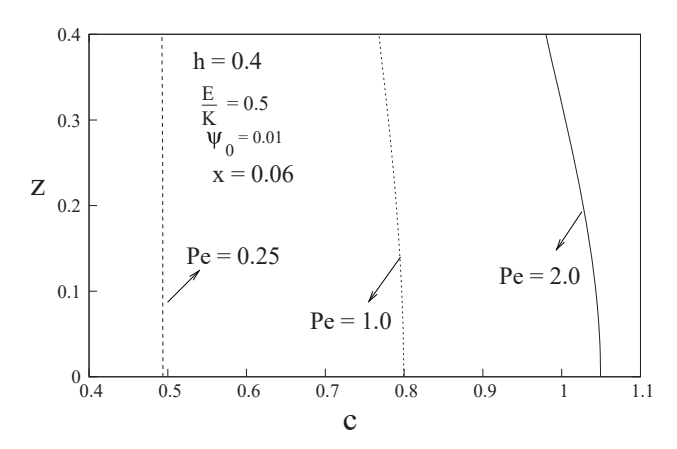


Figure 5: Distribution of concentration c with z for different values of Peclet number Pe.

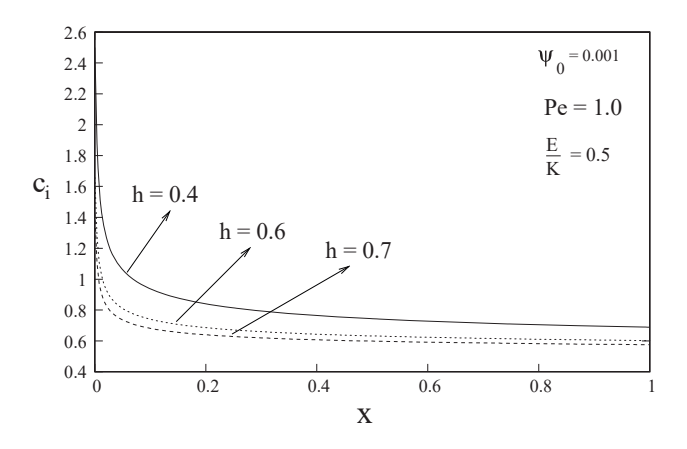


Figure 6: Distribution of concentration at the interface c_i for different heights.

Squeeze film pressure (p):

Axial distribution of squeeze film pressure p with x for various values of h is shown in Figure 7. The general pattern is that p increases as h decreases. It may be noted

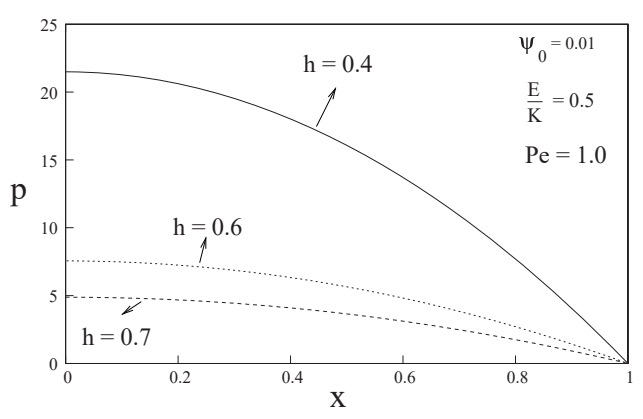


Figure 7: Distribution of pressure p with x for different values of h.

that when the gap between two articular surfaces decreases, there is a resistance to sideways flow and further, the viscosity of the fluid increases due to increase in concentration of HA in the film region. Because of these reasons, squeeze film pressure increases as the gap decreases.

Figure 8 shows the effect of variation of permeability parameter ψ_0 on squeeze film pressure p with respect to x. The effect of surface permeability is to decrease the pressure in the film region. As permeability of the cartilage surface increases, HA and synovial fluid can easily move through the surface. Hence, viscosity of the fluid decreases due to decrease in concentration of acid molecules and also the amount of fluid retained in the film region is small which in turn decrease the squeeze film pressure.

Figure 9 represents the distribution of squeeze film pressure p with x for various values of elastic parameter E/K. The general profile is that p increases with increasing values of E/K. As mentioned earlier, the values of E/K for normal and degenerative articular cartilage are 0.6 and 0.2,

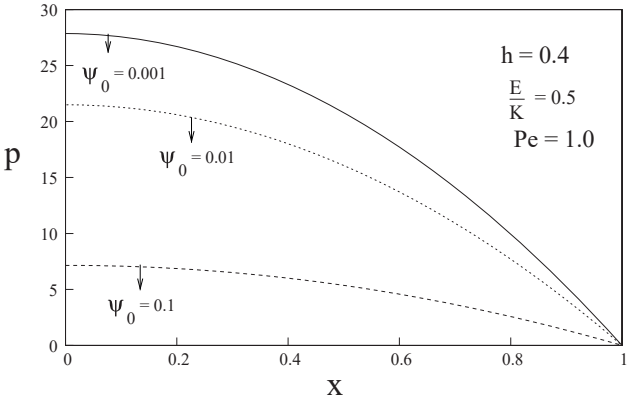


Figure 8: Distribution of pressure p with x for different values of ψ_0 .

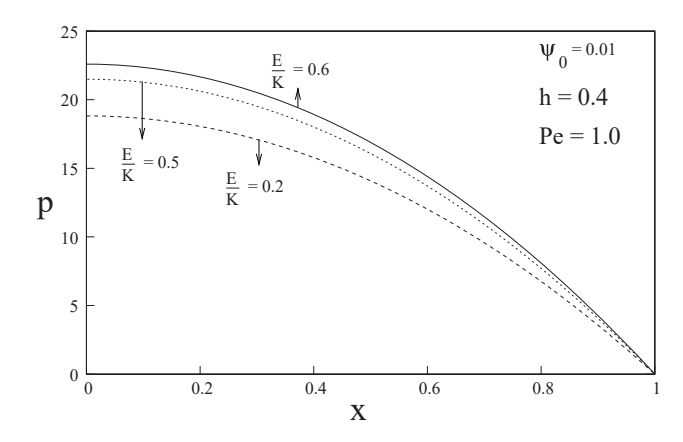


Figure 9: Distribution of pressure p with x for different values of E/K.

respectively. Therefore, joint with normal cartilage surface may have more pressure in comparison with degenerative cartilage surface.

Load carrying capacity (W):

Variation of load carrying capacity W with film height h for different values of λc_0 is shown in Figure 10. Decrease in the height between two surfaces increases the load carrying capacity. This may be explained that as the height of the film region decreases the pressure distribution increases and hence the load carrying capacity increases. Further, the load carrying capacity increases as λc_0 increases. In other words, the load carrying capacity increases with increased values of concentration of solute particles in the film region.

Figures 11 and 12 depict the variation of W with h for different values of ψ_0 and E/K, respectively. It is observed that W decreases as ψ_0 increases, from $\psi_0 = 0.001$ and $\psi_0 = 0.1$. Due to more permeability of the poroelastic surface, the pressure in the film region

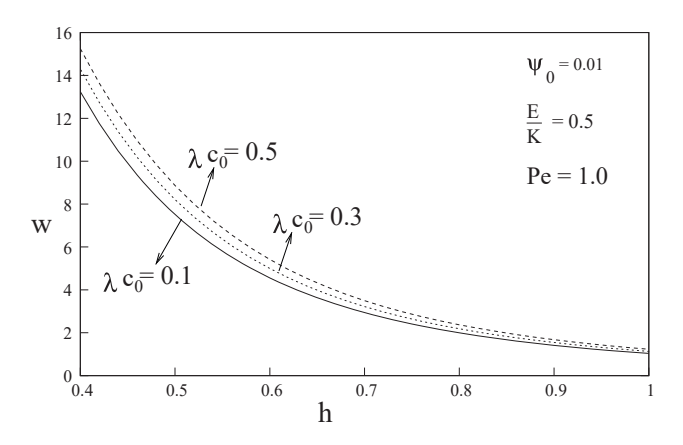


Figure 10: Variation of load carrying capacity W at various heights h for different values of λc_0 .

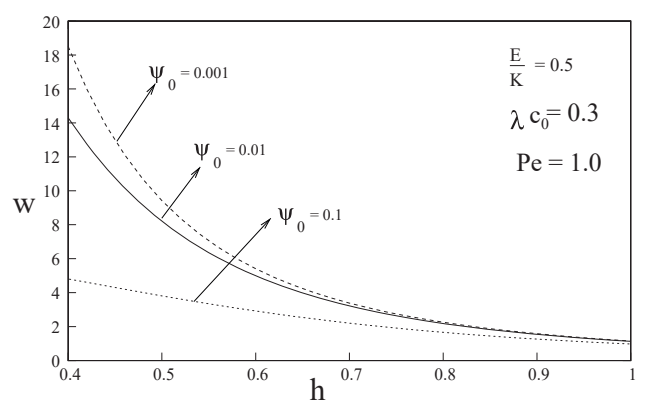


Figure 11: Variation of load carrying capacity W at various heights h for different values of ψ_0 .

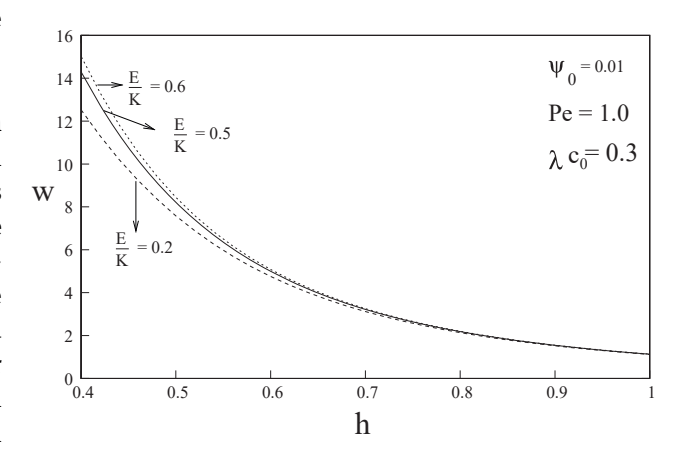


Figure 12: Variation of load carrying capacity W at various heights h for different values of E/K.

decreases and consequently the load carrying capacity decrease. Further, W increases with increasing values of E/K.

5 Conclusion

In this paper, a mathematical model has been proposed to study the squeeze film lubrication by taking into account the permeability, elasticity of the bearing surfaces and the viscosity variation of the lubricant due to change in the concentration of solute particles.

- (1) It is found that the squeeze film pressure and the load carrying capacity increase as the concentration of solute particle increases.
- (2) Further the concentration of solute particles, squeeze film pressure and load carrying capacity increase as the elastic parameter increases but they decrease with increase in the permeability.

(3) The results obtained for various values of parameter *h* show a strong influence on the concentration of solute particles and the film pressure.

References

- [1] N. M. Bujurke and R. B. Kudenatti, "An analysis of rough poroelastic bearings with reference to lubrication mechanism of synovial joints," Appl. Math. Comput., vol. 178, pp. 309-320, 2006.
- [2] Peeyush Chandra, Mathematical Model for Synovial Joints A Lubrication Biomechanical Study, PhD Thesis, IIT Kanpur, 1975.
- [3] P. A. Torzilli and V. C. Mow, "On the fundamental fluid transport mechanisms through normal and pathological articular cartilage during functon-II - The analysis, solution and conclusions," J. Biomech., vol. 9, pp. 587-606, 1976.
- [4] N. M. Bujurke, M. Jagadeeswar, and P. S. Hiremath, "Analysis of normal stress effects in a squeeze film porous bearing," Wear, vol. 116, pp. 237-248, 1987.
- [5] J. S. Hou, V. C. Mow, W. M. Lai, et al. "An analysis of the squeezefilm lubrication mechanism for articular cartilage," J. Biomech., vol. 25, no. 3, pp. 247-259, 1992.
- [6] P. N. Tandon, N. H. Bong, and Kushwaha Kiran, "A new model for synovial joint lubrication," Int. J. Bio Med Comput. vol. 35, no. 2, pp. 125-140, 1994.
- [7] N. M. Bujurke and R. B. Kudenatti, "Surface roughness effects on squeeze film poroelastic bearings," Appl. Math. Comput., vol. 174, pp. 1181-1195, 2006.
- [8] P. S. Walker, D. Dowson, M. D. Longfield, and V. Wright, "Boosted lubrication in synovial joints by fluid entrapment and enrichment," Ann. Rheum. Dis., vol. 27, pp. 512-522, 1968.
- [9] A. S. Tannin, S. G. Nicholas, T. N. Quynhhoa, et al. "Boundary lubrication of articular cartilage - role of synovial fluid constituents," Arthritis Rheumatol., vol. 56, no. 3, pp. 882-891,
- [10] Richard Collins, "A model of lubricant gelling in synovial joints," J. Appl. Math. Phys., vol. 33, pp. 93-123, 1982.
- [11] P. N. Tandon, P. Nirmala, T. S. Pal, et al. "Rheological study of lubricant gelling in synovial joints during articulation," Appl. Math. Model., vol. 12, pp. 72-74, 1988.
- [12] M. Alshehri and S. K. Sharma, "Computational model for the generalised dispersion of synovial fluid," IJACSA, vol. 8, no. 2, pp. 134-138, 2017.
- [13] P. Pustejovska, "Mathematical modeling of synovial fluids flow," WDS'08 Proceedings of Contributed papers, Part III, pp. 32–37, 2008.

- [14] J. Hron, J. Malek, P. Pustejovska, et al. "On the modeling of the synovial fluid," Adv. Tribol., pp. 1-12, 2010.
- [15] E. R. Morris, D. A. Rees, and E. J. Welsh, "Conformation and dynamic interactions in hyaluronate solutions," J. Mol. Biol., vol. 138, no. 2, pp. 383-400, 1980.
- [16] P. S. Walker and M. J. Erkman, "Metal-on-metal lubrication in artificial human joints," Wear, vol. 21, pp. 377-392, 1972.
- [17] O. Pinkus and B. Sternlicht, Theory of Hydrodynamic Lubrication, New York, McGraw-Hill, 1961.
- [18] N. B. Naduvinamani and G. K. Savitramma, Effect of Surface Roughness on the Squeeze Film Lubrication of Finite Poroelastic Partial Journal Bearing with Couple Stress Fluids: A Special Reference to Hip Joint Lubrication, ISRN Tribology, 2014. nn. 1-13.
- [19] J. Ferguson, J. A. Boyle, R. N. M. Mcsween, et al. "Observations on the flow properties of the synovial fluid from patients with rheumatoid arthritis," Biorheology, vol. 5, no. 2, pp. 119-131, 1968.
- [20] R. Y. Hori and L. F. Mockros, "Indentation tests of human articular cartilage," J. Biomech., vol. 9, no. 4, pp. 259-268, 1976.
- [21] U. R. Shettigar, H. J. Prabhu, and D. N. Ghista, "Blood ultrafiltration: A design analysis." Medi. Biol. Engg. Comput., vol. 15, no. 1, pp. 32-38, 1977.
- [22] J. Prakash and S. K. Vij, "Load capacity and time-height relations for squeeze films between porous plates," Wear, vol. 24, pp. 309-322, 1973.
- [23] T. J. Chung, Computational Fluid Dynamics, 2nd ed. Cambridge University press, 2010.
- [24] Tamer Mahmoud Tamer, "Hyaluronan and synovial joint: function, distribution and healing," Interdiscipl. Toxicol., vol. 6, no. 3, pp. 111-125, 2013.
- [25] M. M. Temple-Wong, B. Hansen, M. Grissom, et al., "Effect of knee osteoarthritis on the boundary lubricating molecules and function of human synovial fluid," Trans. Orthop. Res. Soc., vol. 35, pp. 340, 2010.
- [26] L. B. Dahl, I. M. Dahl, A. Engstrom-Laurent, et al. "Concentration and molecular weight of sodium hyaluronate in synovial fluid from patients with rheumatoid arthritis and other arthropathies," Ann. Rheum. Dis, vol. 44, pp. 817-822, 1985.
- [27] A. Maroudas, "Hyaluronic acid films," Proc. Inst. Mech. Eng., vol. 181, pp. 122-124, 1967.
- [28] P. S. Walker, J. Sikorski, D. Dowson, et al. "Behaviour of synovial fluid on surfaces of articular cartilage - A scanning electron microscope study," Ann. Rheum. Dis., vol. 28, pp. 1-14, 1969.